Research article

Journal of RAMAN SPECTROSCOPY

Received: 19 April 2012 Revised: 6 June 2012 Accepted: 10 June 2012 Published online in Wiley Online Library: 16 July 2012

(wileyonlinelibrary.com) DOI 10.1002/jrs.4145

Enhanced Fröhlich interaction of semiconductor cuprous oxide films determined by temperature-dependent Raman scattering and spectral transmittance

Wenlei Yu, Meijie Han, Kai Jiang, Zhihua Duan, Yawei Li, Zhigao Hu* and Junhao Chu

Anomalous low temperature behaviors in cuprous oxide (Cu_2O) film grown on quartz substrate have been investigated by temperature-dependent Raman and transmittance spectra. The longitudinal optical components of two Γ_{15}- phonon modes become sharper and more intense at a low temperature. It can be found that the highest-order electronic transition located at 6.4 eV exhibits a minimum transmittance near 200 K. Correspondingly, the variations from phonon intensity ratios reveal obvious anomalies with the decreasing temperature, indicating the existence of strong electron–phonon coupling mediated by Fröhlich interaction in the Cu_2O films below the temperature of 200 K. Copyright © 2012 John Wiley & Sons, Ltd.

Keywords: cuprous oxide; Fröhlich interaction; Raman spectroscopy

Introduction

Cuprous oxide (Cu_2O) is a *p*-type semiconductor with a direct band gap of 2.17 eV and also displays well-defined series of excitonic features in the absorption and luminescence spectra with the large excitonic binding energy (150 meV).[1–3] Even though Cu_2O is known for decades, the material has recently drawn renewed interest for the conversion of solar energy into electrical or chemical energy, showing a theoretical solar efficiency of about 9–11%.[4] As one of the most key candidates for solar cell material, the optical properties and crystalline quality influence both the heat losses and gains.[5] Therefore, it is necessary to prepare pure Cu_2O nanocrystals to further examine the crystal structure and characterize the electronic properties. It can be found that Raman spectra from Cu_2O material provide some anomalies for the thermal behavior at 90 and 180 K, which might be related to structural and/or electronic changes.[6] However, the experimental phenomena cannot be reproduced from temperature dependence of the lattice constant, where the reversible anomaly associated with the thermal expansion is close to 200 K.[6] Additionally, negative thermal expansion (NTE) behavior of cubic Cu_2O has been calculated, which is in fair agreement with the available experimental data up to 200 K.[7] The origin of the discrepancies between theoretical and experimental results for NTE as well as Hall mobilities at temperatures above 200 K is currently unresolved.[7,8] These phenomena make us pay attention to the variation on physical picture from Cu_2O as a function of temperature, especially for the vicinity of 200 K.

Raman scattering has been known to be an excellent nondestructive tool to study the crystal structure, chemical composition, and lattice dynamics of various materials. Generally, Cu_2O possesses three acoustic and 15 optical branches with infrared-active symmetry $\Gamma_{15-}{}^{(1)}$, $\Gamma_{15-}{}^{(2)}$, Raman-active Γ_{25+}, and other symmetry selection rule forbidden modes (Γ_{25-}, Γ_{2+}, and Γ_{12-}). The forbidden modes were allowed through defects or in an intrinsic selection rule violation mechanism in the pure crystal.[6] Moreover, scattering at grain boundaries and size effect could be also contributed to the Raman information on the crystal structure for Cu_2O material. Lattice dynamical calculations show that Cu-dominated modes are responsible for the low frequency part, whereas modes above 60 meV (484 cm^{-1}) are oxygen dominated.[7,9] The copper site exhibits a preferential vibration in the direction perpendicular to the linear O–Cu–O bond. This could explain the NTE through the rotation of Cu_4O tetrahedra, which can shorten O–O distance.[10] Bohnen *et al.* describe the NTE behavior below 300 K and the origin is because of anomalous behavior of phonon modes with energy less than 20 meV (162 cm^{-1}), which is a highly sensitive wave vector.[9] Note that the thermal expansion is related to phonon dispersion, and Raman spectra can provide some invaluable information on the crystal structure for Cu_2O material. In addition, temperature dependence of the electronic transitions can also be directly correlated to the band structure of semiconductor Cu_2O material. It plays a supporting role in analysis of physical properties behind the anomalous behavior. Moreover, little work has been carried out to investigate the higher energy electronic transitions from the cuprite structure up to date. Therefore, it is desirable to carry out a detail study regarding the essential effects of temperature

* *Correspondence to: Zhigao Hu, Key Laboratory of Polar Materials and Devices, Ministry of Education, Department of Electronic Engineering, East China Normal University, Shanghai 200241, China. E-mail: zghu@ee.ecnu.edu.cn*

Key Laboratory of Polar Materials and Devices, Ministry of Education, Department of Electronic Engineering, East China Normal University, Shanghai 200241, China

Journal of RAMAN SPECTROSCOPY

on lattice vibrations and high energy transitions, in order to detect possible anomalies in the Cu_2O structure

Experimental

Nanocrystalline Cu_2O film studied in this work was prepared on quartz substrate by the sol–gel method.[11] Copper acetate hydrate $[Cu(C_2H_3O_2)_2\,H_2O$, 99%, 0.4 g] was dissolved in anhydrous ethanol (C_2H_6O, 99.7%, 20 ml) under magnetic stirring. After the solution was stable and became transparent and homogeneous, the 0.1-M precursors were spin-coated onto quartz substrate at the speed of 4000 rpm for 20 s. The deposited film was dried at 300 °C for 300 s to remove residual organic compounds, following annealed at 800 °C for 15 min in N with a flow of 2.0 l/min by a rapid thermal annealing procedure. It should be emphasized that the films deposited from the sol–gel process generally consist of dense film layer and surface rough layer (SRL), which maybe contain a large void fraction. The obtained void component is about 1.2% for the SRL, which indicates that the SRL contains a small void fraction and the present Cu_2O film with the thickness of about 100 nm is relatively dense with the aid of spectroscopic ellipsometry measurement.

The crystalline structure of the film was analyzed by using X-ray diffraction (XRD, D/MAX-2550 V, Rigaku Co.). There are two diffraction peaks observed from the XRD pattern (not shown), which indexed to the (111) and (200) peaks of cubic Cu_2O. No characteristic XRD peaks arising from impurities that are detected, indicating that the sample is composed of pure Cu_2O phase. From the diffraction angle and the full width at half-maximum of the (200) peak, the average crystallite size is calculated to be about 24 nm using the well-known Scherrer's equation and the lattice parameter of *a* is estimated to be 4.251 Å. It should be pointed out that the XRD measurement reflects the crystalline domain size rather than the physical particle size, suggesting that the obtained particles may contain multi-domains with the particle or polycrystalline particles.[12] Furthermore, the *a* value is slightly smaller than those reported (4.27 Å) in Cu_2O films electrodeposited on three substrates (Si, ITO, and Au).[12] This discrepancy can be ascribed to different sublattice mismatch, stress, and/or strain, which can be normally affected by the deposition technique and substrate material. From Hall measurements by ver der Pauw method at room temperature (RT), the carrier charge in the Cu_2O film is found to be positive, showing the *p*-type behavior with Hall mobility of 31.7 $cm^2V^{-1}\,s^{-1}$. It is slightly less than that (35 $cm^2V^{-1}\,s^{-1}$) of the Cu_2O films obtained by pulsed laser deposition.[13] The carrier concentration is about $2.05 \times 10^{14}\,cm^{-3}$ and the resistivity is $9.61 \times 10^2\,\Omega cm$. In order to further confirm the crystallinity, composition and structure of the Cu_2O film, Raman scattering was carried out by a Jobin-Yvon LabRAM HR 800 ultraviolet (UV) micro-Raman instrument with a He–Ne (633 nm) laser and an Ar^+ (488 nm) laser as excitation sources. The sample was mounted into a Linkam THMSE 600 heating stage for variable temperature experiments (77–300 K). The transmittance spectra at different temperatures (8–300 K) were recorded over the photon energy range from 0.47 to 0.65 eV using a double beam UV-infrared spectrophotometer (PerkinElmer Lambda 950) and an optical cryostat (Janis SHI-4-1). Note that the effects of the annealing step on the Raman scattering for the Cu_2O films deposited under different annealing temperature (800, 850, and 900 °C) are not remarkable. It suggests that the films grown under higher annealing temperature are unlikely to undergo further oxidation and the films are relatively stable as the Cu_2O phase.[14] Therefore, the film annealed at 800 °C was chosen for the temperature dependence studies in the present work.

Results and discussion

Fig. 1(a, b) shows the Raman scattering of the Cu_2O film with the laser lines of 488 and 633 nm. The Raman spectrum at a temperature of 77 K is chosen for the frequency studies and the features generating from zone-center phonon are identified as follows:[6,15,16] Γ_{25-} (81 cm^{-1}), Γ_{12-} (106 cm^{-1}), $\Gamma_{15-}^{(1)}$ (longitudinal-optical (LO)-phonon frequency, 150 cm^{-1}), $2\Gamma_{12-}$ (215 cm^{-1}), $2\Gamma_{15-}^{(1)}$ (304 cm^{-1}), $4\Gamma_{12-}$ (415 cm^{-1}), Γ_{25+} (505 cm^{-1}), $\Gamma_{15-}^{(2)}$ (transverse-optical (TO)-phonon frequency, 632 cm^{-1}; LO, 655 cm^{-1}), $\Gamma_{15-}^{(1)}$ (LO) + $\Gamma_{15-}^{(2)}$ (LO) (810 cm^{-1}). The sharp peaks of the infrared-allowed mode $\Gamma_{15-}^{(1)}$ (LO, 151 cm^{-1}) and second-order overtone $2\Gamma_{12-}$ (215 cm^{-1}) indicate the existence of strong electron–phonon coupling mediated by Fröhlich interaction in the film composed of the Cu_2O phase.[17] Other weak scattering from Raman forbidden first-order modes such as those at 106, 632, and 655 cm^{-1} could be due to intrinsic selection rule violation mechanisms in pure Cu_2O crystal.[15] The low frequency vibration mode Γ_{25-} (81 cm^{-1}) represents a rigid rotation of the Cu_4O tetrahedron around oxygen atoms, arising from the transverse vibration of Cu atoms, which partially contributes to the NTE.[7,18] Although the phonon mode at 106 cm^{-1} is a twisting of the Cu_4O tetrahedron around the *c* axis, it also leads to the NTE because of the tension mechanism of the O–Cu–O bonds.[18] The only Raman-active mode Γ_{25+} (505 cm^{-1}) is assigned to relative motion of the two simple cubic O lattices. It can participate in one-phonon non-resonant Raman scattering because of parity selection rules and appear at the same frequency for different excitations (488 and 514.5 nm).[6] For the excitation source using 633 nm in the present case, the spectrum of the Cu_2O material from Fig. 1(b) displays only two prominent peaks around 148 and 222 cm^{-1}. The deviation compared with those excited by 488 nm laser at RT suggests that the two peaks cannot be ascribed to luminescence. Note that several

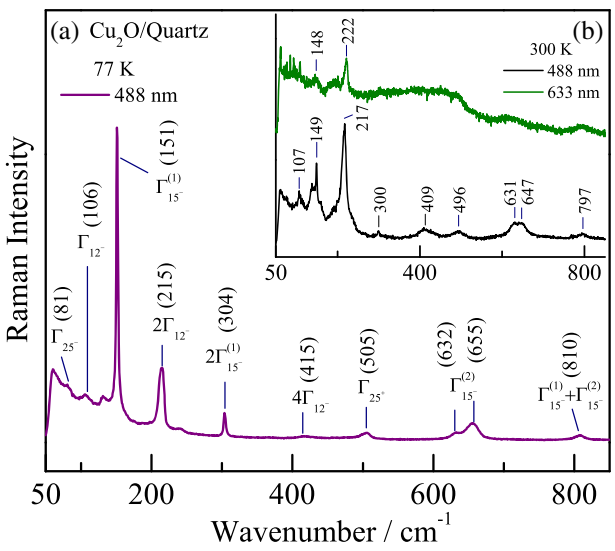

Figure 1. (a) Raman spectrum excited by 488-nm laser for the Cu_2O film on the quartz substrate at 77 K. (b) A comparison of Raman scattering with 488 and 633-nm laser excitations at room temperature. The corresponding phonon modes are uniquely assigned.

Raman peaks in the region of 50–850 cm^{-1} are distinct and enhanced with the application of 488 nm. The result can be explained by the fact that the 488 nm excitation (2.54 eV) is in near-resonance with the band gap energy of the Cu_2O film, then the selection rule is broken and the Raman signal reveals large enhancement.[17,19] Therefore, all of the Raman data show typical phonon vibrations of Cu_2O crystal and support the formation of Cu_2O, which is also in agreement with the XRD experiments.

Fig. 2 describes the temperature-dependent Raman scattering for the Cu_2O layer on quartz substrate. The only allowed-Raman phonon mode Γ_{25+}, which can be attributed to interband scattering via the deformation-potential interaction,[17] presents softening and broadening trend at a high temperature. The mode also has a remarkable redshift of 9 cm^{-1} with increasing the temperature from 77 K to RT. Experimentally, it was found that the Γ_{12-} phonon has the strongest coupling to the yellow exciton.[20] In the 488 nm excitation, the Γ_{12-} (106 cm^{-1}), $2\Gamma_{12-}$ (215 cm^{-1}), and $4\Gamma_{12-}$ (415 cm^{-1}), neither infrared nor Raman mode, can be observed. The most intense Raman signal at RT is the second-order overtone $2\Gamma_{12-}$; but at the lowest temperature, infrared-allowed mode $\Gamma_{15-}{}^{(1)}$ (LO, 151 cm^{-1}) develops the maximum intensity. Additionally, with increasing the temperature, the $\Gamma_{15-}{}^{(1)}$ (LO) mode shifts to a low energy side, but the $2\Gamma_{12-}$ has an opposite variation. At a temperature of 77 K, the intensity of $\Gamma_{15-}{}^{(1)}$ (LO) is approximately four times as that of $2\Gamma_{12-}$ mode. Then, the intensity ratio for I_{151}/I_{215} abruptly decreases until the temperature rises up to 200 K. With the temperature further increasing, the ratio is less than unity, suggesting that the intensity of $\Gamma_{15-}{}^{(1)}$ (LO) is weaker than that of $2\Gamma_{12-}$ at a high temperature. The similar phenomena from I_{304}/I_{415} can be also observed and indicate the emergence of the structural or electronic transition near the special temperature (T_A) of 200 K. For comparison, the corresponding ratios of I_{304}/I_{415} are smaller than the ones for I_{151}/I_{215} at a low temperature region because of the second-order response. It is reasonable that the variation of I_{304}/I_{415} shares with the same behavior for I_{151}/I_{215} with the temperature.

The polar mode Γ_{15-} is of particular interest because the LO phonon carries an electric field, associated with Fröhlich interaction, which produces the LO–TO splitting and leads to additional scattering for the LO component. The 2.5 cm^{-1} splitting of the lower frequency $\Gamma_{15-}{}^{(1)}$ mode has been reported.[21] In the present works, however, it is impossible to separate the two peaks unambiguously from the $\Gamma_{15-}{}^{(1)}$ mode. The extracted energy (151 cm^{-1}, 18.7 meV) for only LO scattering $\Gamma_{15-}{}^{(1)}$ (LO) at 77 K is slightly less than the reported value of 19.1 meV at 10 K.[22] On the other hand, it can be found that the $\Gamma_{15-}{}^{(2)}$ (TO) mode is almost unchanged and the $\Gamma_{15-}{}^{(2)}$ (LO) largely shifts to low frequency with increasing the temperature. The maximum deviation of about 13 cm^{-1} obtained for the 810-cm^{-1} mode is close to the sum of the shifts from $\Gamma_{15-}{}^{(1)}$ (LO) to $\Gamma_{15-}{}^{(2)}$ (LO) in the temperature range, which is affected by the thermal effect. Moreover, the LO–TO splitting (23 cm^{-1}) from the $\Gamma_{15-}{}^{(2)}$ mode at 77 K is slightly smaller than that reported by Genack (30 cm^{-1} at 4 K).[21] It indicates that the vibrations related with the Fröhlich interaction are sensitive to the temperature. In the absence of the Fröhlich interaction, the Raman constants for LO and TO scattering would be identical.[21] It can be deduced that the larger splitting value means the stronger Fröhlich mechanism to Raman scattering. Additionally, the sharper LO component at a low temperature could be found in Fig. 2. This is because the macroscopic electric field associated with the $\Gamma_{15-}{}^{(2)}$ (LO) is rather strong and the exciton–phonon interaction will be predominant of the Fröhlich type rather than deformation-potential type.[20] Furthermore, the TO and LO components of the $\Gamma_{15-}{}^{(2)}$ become more difficult to be distinguished and the ratio of the intensity (I_{655}/I_{632}) nearly approaches to 1 in the range of 210 K RT. The coexistence of Fröhlich and deformation-potential contributions is responsible for the adjustment of phonon modes and results in similar intensity of the TO and LO modes for the Cu_2O film.

The temperature evolutions of the intensity ratios for the I_{151}/I_{215}, I_{304}/I_{415}, and I_{655}/I_{632} are plotted in Fig. 3. The anomalous behavior can be easily recognized based on the abrupt variations with the temperature. The singularities take place at T_A of 200 K

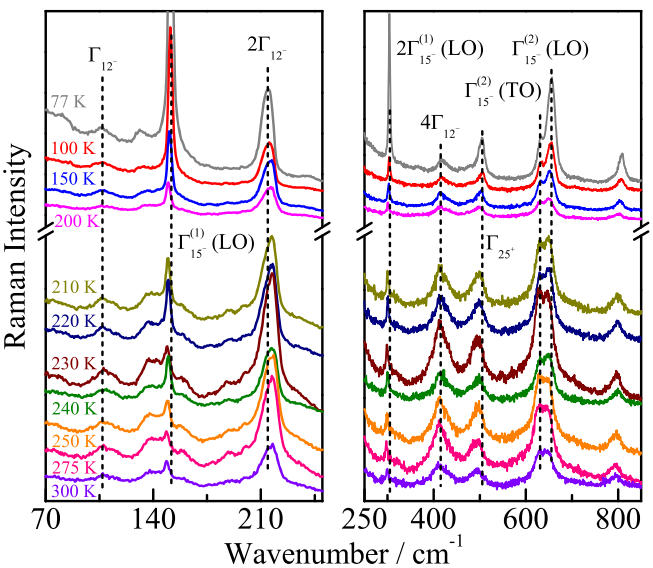

Figure 2. Temperature dependence of Raman scattering for the Cu_2O film with 488-nm excitation from 77 to 300 K. The phonon modes have been marked and the dashed lines represent the shift to guide the eyes.

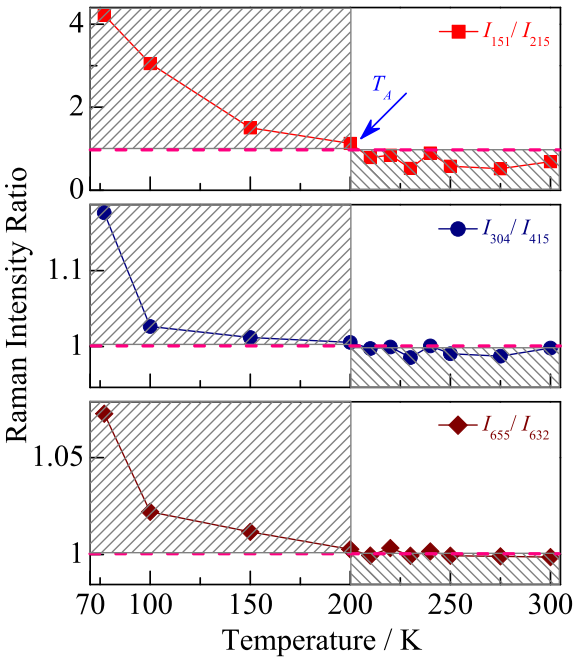

Figure 3. Raman intensity ratios from I_{151}/I_{215}, I_{304}/I_{415}, and I_{655}/I_{632} as a function of temperature for the Cu_2O film. The bar with oblique lines indicates the anomalies in the vicinity of the special temperature (T_A).

Journal of RAMAN SPECTROSCOPY

from the Raman scatting for the Cu_2O film. In addition, the T_A in the temperature dependence of lattice constant for Cu_2O material during both cooling and heating processes has been recorded.[6] It is also reported that the cell parameter a of Cu_2O decreases when the temperature is varied from liquid helium temperature to 200 K and remains virtually constant from 200 to 300 K.[23] From the variations of the three ratios, with increasing the temperature, all values have a remarkable reduction at the temperature and almost keep unity in the range of 210 K RT. It indicates the importance of the Fröhlich and deformation-potential interactions for Raman spectra of the cuprite structure, especially for the polar mode Γ_{15-}. Therefore, one can conclude that the Fröhlich interaction can be assumed as the dominant factor in the Raman scattering below the T_A, which will cause the two LO components of the Γ_{15-} modes to be sharper and more intense. Passing T_A and at a high temperature, Fröhlich and deformation-potential types together induce the crystal structure modifications and further affect the optical properties. Furthermore, it was reported that the carriers begin to freeze out below 220 K from the change of the carrier concentration with temperature for a Cu_2O layer grown on MgO substrate.[24] It was also argued that the Hall mobility becomes limited by the carrier scattering from ionized centers at low temperatures.[8] Shimada and Masumi revealed the Hall mobility of Cu_2O when it is limited by LO phonon modes with 220 K and mobility quenching because of the metastable self-trapping of holes, which possibly result in the unusual phenomena above 200 K.[8,25] The similar anomaly at about 200 K suggests that the variation of free carrier concentration with the temperature could play an important role in broadening and softening the Fröhlich optical phonons of the Cu_2O film.

On the other hand, transmittance spectra collected at 8, 80, 200, 250 and 300 K for the Cu_2O film are displayed in Fig. 4. As can be seen, two prominent shoulders appear at near 2.58 and 2.7 eV, even remain at RT, which result from transitions to excitonic levels. The former features between the peculiar second-lowest conduction band Γ_8^- and the split valence bands (an upper Γ_7^+ band and a lower Γ_8^+ band) can be regarded as blue ($\Gamma_7^+ \rightarrow \Gamma_8^-$) and indigo ($\Gamma_8^+ \rightarrow \Gamma_8^-$) exciton states, respectively, which are direct and allowed.[26,27] The difference between them is estimated to be about 120 meV and very close to the split value ($_{SO}$ = 124 meV) because of the spin–orbit interaction.[27] Moreover, the major structures in higher energy located at 3.45, 4.27, and 5.41 eV can be accounted for specific band-to-band transitions. The broadening bands in order are ascribed to $X_3 \rightarrow X_1$, $M_1 \rightarrow M_1$, and $R_{25}' \rightarrow R_{15}$ transitions of Cu_2O, respectively.[27,28] Some additional bands between 4.27 and 5.41 eV, corresponding to a complex electronic structure, become much stronger at the lowest temperature. It is found that these UV bands may be assigned to the transitions from the copper d-shells to the higher sublevels of conduction band.[29] And absorption in the 215–250 nm (5.76–4.96 eV) range has been characterized by the 3d–4s transition of isolated Cu^+ ions.[30] From the insets of Fig. 4, the shift of the UV absorption bands with the temperature is relatively large in comparison with that for the blue and indigo bands of excitonic series. The narrow widths of the blue and indigo lines at a low temperature indicate the semiconductor nature of the direct-allowed exciton transitions.[27] In addition, the intensity reduction for all the dips mentioned earlier can be observed as the temperature increases, showing a remarkable response to the temperature. However, the highest-order transition at about 6.4 eV, which is described by an interband transition from the occupied Cu 3d state to the unoccupied states with mixed Cu 3d, 4s, and O 2p character,[31] does not follow a regular relationship with the temperature. Interestingly, the intensity of the peak or dip in the range of 5.7–6.5 eV exhibits a large decrease with increasing the temperature in the spectral transmittance, then the minimum can be obtained for the temperature of 200 K. It indicates that the change in the crystalline and electronic band structure occurs as the temperature is near 200 K. The finding is similar to the anomalous temperature from Raman scattering mentioned earlier. It should be emphasized that the present Cu_2O film has polycrystalline formation and is composed of crystallites with an average size of 24 nm, as indicated by the XRD pattern. The grain size for the low dimensional system may affect the electronic transition and the optical response. So, it is possible that the confinement effect can influence the electronic band structure variations and results in the unusual transmittance with the temperature for the Cu_2O nanocrystalline film. On the other hand, the void component is about 1.2% for the SRL with several nanometers, whose contributions are tiny compared with the thickness of the film (100 nm). Moreover, the relatively big light spot (about 4 mm in diameter) and normal-incident configuration, which cannot be sensitive to porous surface layer and/or void density, are applied in the present transmittance experiments. It indicates that the void contribution effects can be neglected for the evaluation of the optical properties in the Cu_2O film. It is pointed out that an average transmittance of about 29% at photon energy higher than 5.7 eV can be observed because of the strong absorption for the Cu_2O film. Nevertheless, the dip value located at 6.4 eV is very close to that reported by spectroscopic ellipsometry measurements in an extended spectral range up to 10 eV.[32] Hence, the observation of the anomalies in transmittance curves further supports the character of the variations from the Raman intensity ratios for the Cu_2O film.

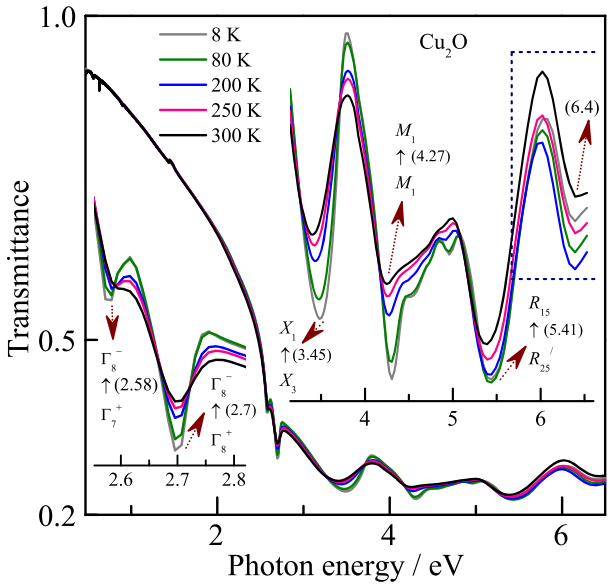

Figure 4. Transmittance spectra of the Cu_2O film were recorded at the temperatures of 8, 80, 200, 250, and 300 K, respectively. For clarity, the enlarged photon energy regions of 2.55–2.82 and 3.15–6.6 eV and transition origins from the band structures are plotted in the insets, respectively. Note that an anomalous transmittance variation in the photon energy region of 5.7–6.5 eV occurs near 200 K. This figure is available in colour online at wileyonlinelibrary.com/journal/jrs

Conclusions

In conclusion, several singularities corresponding to different electronic transitions can be clearly identified from the transmittance spectra of the Cu_2O film in the photon energy range of 0.47–6.5 eV and there is a minimum transmittance at 200 K for the highest-order transition located at 6.4 eV. The temperature-dependent Raman intensity ratios of the I_{151}/I_{215}, I_{304}/I_{415}, and I_{655}/I_{632} have been investigated and the anomalous behaviors in the vicinity of 200 K can be found. The dominant contributions to the enhancement of Raman scattering can be ascribed to strong Fröhlich mechanism at a low temperature.

Acknowledgements

This work was financially supported by the Major State Basic Research Development Program of China (Grant No. 2011CB922200), Natural Science Foundation of China (Grant Nos. 11074076, 60906046, and 61106122), Projects of Science and Technology Commission of Shanghai Municipality (Grant Nos. 11520701300,10DJ1400201, and 10SG28), and the Program for Professor of Special Appointment (Eastern Scholar) at Shanghai Institutions of Higher Learning. One of the authors (Wenlei Yu) thanked the support from the Project of East China Normal University (Grant No. CX2011005).

References

[1] R. Hassanien, S. A. F. Al-Said, L. Siller, R. Little, N. G. Wright, A. Houlton, B. R. Horrocks, *Nanotechnology* **2012**, *23*, 075601.
[2] K. Suzuki, N. Tanaka, A. Ando, H. Takagi, *J. Am. Ceram. Soc.* **2011**, *94*, 2379.
[3] K. Das, S. N. Sharma, M. Kumar, S. K. De, *J. Appl. Phys.* **2010**, *107*, 024316.
[4] W. Y. Zhao, W. Y. Fu, H. B. Yang, C. J. Tian, M. H. Li, Y. X. Li, L. N. Zhang, Y. M. Sui, X. M. Zhou, H. Chen, G. T. Zou, *Cryst. Eng. Comm.* **2011**, *13*, 2871.
[5] X. D. Xiao, L. Miao, G. Xu, L. M. Lu, Z. M. Su, N. Wang, S. Tanemura, *Appl. Surf. Sci.* **2011**, *257*, 10729.
[6] M. Ivanda, D. Waasmaier, A. Endriss, J. Inhringer, A. Kirfel, W. Kiefer, *J. Raman Spectrosc.* **1997**, *28*, 487.
[7] R. Mittal, S. L. Chaplot, S. K. Mishra, P. P. Bose, *Phys. Rev. B* **2007**, *75*, 174303.
[8] Y. S. Lee, M. T. Winkler, S. C. Siah, R. Brandt, T. Buonassisi, *Appl. Phys. Lett.* **2011**, *98*, 192115.
[9] K.-P. Bohnen, R. Heid, L. Pintschovius, A. Soon, C. Stampfl, *Phys. Rev. B* **2009**, *80*, 134304.
[10] M. Tiano, M. Dapiaggi, G. Artioli, *J. Appl. Crystallogr.* **2003**, *36*, 1461.
[11] M. J. Han, K. Jiang, J. Z. Zhang, Y. W. Li, Z. G. Hu, J. H. Chu, *Appl. Phys. Lett.* **2011**, *99*, 131104.
[12] Y. L. Liu, Y. C. Liu, R. Mu, H. Yang, C. L. Shao, J. Y. Zhang, Y. M. Lu, D. Z. Shen, X. W. Fan, *Semicond. Sci. Technol.* **2005**, *20*, 44.
[13] K. R. Balasubramaniam, V. M. Kao, J. Ravichandran, P. B. Rossen, W. Siemons, J. W. Ager III, *Thin Solid Films* **2012**, *520*, 3914.
[14] F. M. Li, R. Waddingham, W. I. Milne, A. J. Flewitt, S. Speakman, J. Dutson, S. Wakeham, M. Thwaites, *Thin Solid Films* **2011**, *520*, 1278.
[15] D. Powell, A. Compaan, J. R. Macdonald, R. A. Forman, *Phys. Rev. B* **1975**, *12*, 20.
[16] H. Solache-Carranco, G. Juarez-Diaz, A. Esparza-Garcia, M. Briseno-Garcia, M. Galvan-Arellano, J. Martinez-Juarez, G. Romero-Paredes, R. Pena-Sierra, *J. Lumin.* **2009**, *129*, 1483.
[17] N. A. Mohemmed Shanid, M. Abdul Khadar, V. G. Sathe, *J. Raman Spectrosc.* **2011**, *42*, 1769.
[18] A. Sanson, *Solid State Commun.* **2011**, *151*, 1452.
[19] P. Y. Yu, Y. R. Shen, *Phys. Rev. Lett.* **1974**, *32*, 373.
[20] Y. Petroff, P. Y. Yu, Y. R. Shen, *Phys. Rev. B* **1975**, *12*, 2488.
[21] A. Z. Genack, H. Z. Cummins, M. A. Washington, A. Compaan, *Phys. Rev. B* **1975**, *12*, 2478.
[22] M. Jörger, T. Fleck, C. Klingshirn, R. von Baltz, *Phys. Rev. B* **2005**, *71*, 235210.
[23] M. Dapiaggi, W. Tiano, G. Artioli, A. Sanson, P. Fornasini, *Nucl. Instr. Meth. in Phys. Res. B* **2003**, *200*, 231.
[24] S. Eisermann, A. Kronenberger, A. Laufer, J. Bieber, G. Haas, S. Lautenschlager, G. Homm, P. J. Klar, B. K. Meyer, *Phys. Status Solidi A* **2012**, *209*, 531.
[25] H. Shimada, T. Masumi, *J. Phys. Soc. Jpn.* **1989**, *58*, 1717.
[26] W. Y. Ching, Y.-N. Xu, K. W. Wong, *Phys. Rev. B* **1989**, *40*, 7684.
[27] H. Amekura, N. Umeda, Y. Takeda, N. Kishimoto, *Appl. Phys. Lett.* **2006**, *89*, 223120.
[28] A. Nath, A. Khare, *J. Appl. Phys.* **2011**, *110*, 043111.
[29] S. Jana, P. K. Biswas, *Mat. Lett.* **1997**, *32*, 263.
[30] A. Oliver, J. C. Cheang-Wong, J. Roiz, J. M. Hern´ andez, L. Rodriguez-Fernandez, A. Crespos, *Nucl. Instr. Meth. in Phys. Res. B* **2001**, *175–177*, 495.
[31] Y.-J. Kim, J. P. Hill, H. Yamaguchi, T. Gog, D. Casa, *Phys. Rev. B* **2010**, *81*, 195202.
[32] F. Haidu, M. Fronk, O. D. Gordan, C. Scarlat, G. Salvan, D. R. T. Zahn, *Phys. Rev. B* **2011**, *84*, 195203.